Pitch-induced transition of chiral nematic liquid crystals in submicrometer cylindrical cavities

R. J. Ondris-Crawford,[1] M. Ambrožič,[2] J. W. Doane,[1] and S. Žumer[1-3]
[1]*Liquid Crystal Institute and Department of Physics, Kent State University, Kent, Ohio 44242*
[2]*J. Stefan Institute, University of Ljubljana, Jamova 39, Ljubljana, Slovenia*
[3]*Physics Department, University of Ljubljana, Jadranska 19, Ljubljana, Slovenia*
(Received 5 July 1994)

A structural transition in the nematic liquid crystal 4'-pentyl-4-cyanobiphenyl (5CB-βd_2) doped with chiral agents CB15 and CE2, confined to submicrometer cylindrical cavities of alumina membranes, is detected by deuterium nuclear magnetic resonance (^{2}H NMR). These cavities have radii R of 0.1 μm and give tangential anchoring conditions. The ^{2}H NMR spectra reveal a transition from a radially twisted to an axially twisted structure. The radially twisted structure is stable for pitch lengths greater than approximately 1 μm and the axially twisted structure for smaller pitch lengths. For the case of equal bulk elastic constants K_{11}, K_{22}, and K_{33} the dependence of the Frank free energy on the inverse pitch parameter q, saddle-splay elastic constant K_{24}, and the surface anchoring strength W_θ is studied. In the radially twisted structure the free energy as a function of q has a sawtooth shape for fixed K_{24}. The phase diagrams showing the stability of the two phases in the inverse twist versus anchoring space for different values of K_{24}, are calculated. In the weak anchoring regime ($RW_\theta/K < 1$), a periodic reentrance from axially to radially twisted structures is predicted upon increasing qR. A comparison of theoretical and experimental results in this chiral nematic material yields a K_{24} value nearly an order of magnitude smaller than that found in nonchiral nematic phases.

PACS number(s): 61.30.Cz, 64.70.Md, 61.30.Jf, 68.10.Cr

I. INTRODUCTION

Chiral nematic liquid crystals exhibiting a helical deformation of the director field have been of interest for many years for fundamental and practical reasons [1]. The effect of an external electric field on chiral nematic helicoidal and blue phases has been studied in particular by Cohen and Hornreich [2], Hornreich and Strikman [3], and Kitzerow *et al.* [4]. These theoretical and experimental studies were performed mainly on systems, confined to planar geometries, where the director was strongly anchored tangential to the substrate. The practical interest in these systems comes primarily from the supertwist cell [5]. Recently discovered polymer stabilized cholesteric texture displays [6] have stimulated interest in more general geometries.

The effect of a curved confining geometry on chiral nematic liquid crystal structures was first reported by Cladis, White, and Brinkman [7]. Using optical polarizing microscopy, they studied the effect of chirality on structures in supramicrometer capillary tubes with homeotropic anchoring conditions near the nematic–smectic A transition. Lequeux and Kleman [8] studied the helicoidal instability in chiral nematic capillary tubes with homeotropic anchoring. Yang and Crooker [9] studied chiral nematic liquid crystal droplets and Bezič and Žumer studied model structures of chiral nematic liquid crystal in spherical [10] and cylindrical [11] cavities. Optical microscopy was used to identify some confined chiral nematic structures [7–9], while NMR has been used to study the effect of biaxial ordering, self-diffusion, and helix distortion only in bulk chiral nematic liquid crystals [12].

We report a study of chiral nematic liquid crystal confined to submicrometer cylindrical cavities with planar surface anchoring. Deuterium nuclear magnetic resonance (^{2}H NMR) spectra reveal a configuration transition from a slightly twisted axial structure where the twist is along the radial direction, hereafter referred to as a radially twisted-axial (RTA) configuration [Fig. 1(b)],

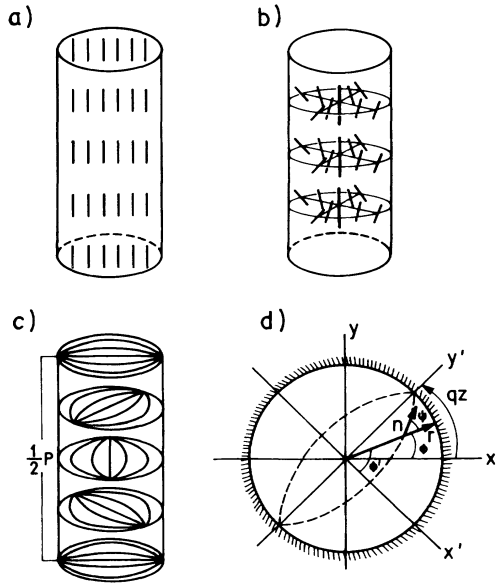

FIG. 1. Nematic director field of (a) the PA configuration, (b) the RTA configuration, (c) the ATPB configuration, and (d) the laboratory and rotating coordinate system for the description of the ATPB configuration.

to a planar structure with a well known bipolar director field whose symmetry axis twists along the cylinder axis, hereafter referred to as an axially twisted planar bipolar (ATPB) configuration [Fig. 1(c)]. Analysis of the Frank free energy shows that the configuration transition depends on the chirality and the polar (out-of-plane) anchoring strength.

II. EXPERIMENT

Studies of nematic 4'-pentyl-4-cyanobiphenyl (5CB) confined to submicrometer cylindrical cavities revealed a planar-bipolar configuration in cavities with the surface enforcing unidirectional (concentric) planar anchoring and with radii less than 0.4 μm [13]. In order to observe a planar structure, therefore, cavity sizes that are much less than the resolution of an optical microscope need to be employed. Deuterium NMR is an effective technique to decipher the distribution of the director field inside submicrometer sized cavities, as long as diffusion averaging can be neglected (deep in nematic phase and $R > 0.1$ μm) [13–15]. The width and the shape of the spectra are determined by the nematic director field inside the cavity and the orientation of the symmetry axis of this configuration with respect to the field. Molecules of a uniaxial compound deuterated at a specific site located in a region of the cylinder represented by the position vector **r**, will yield a spectrum of two lines with angular quadrupole frequency splitting given by the expression [16]

$$\delta\nu(\mathbf{r}) = \tfrac{1}{2}\delta\nu[3\cos^2\theta_n(\mathbf{r}) - 1] , \tag{1}$$

where $\delta\nu$ is the quadrupole splitting of the aligned bulk and $\theta_n(\mathbf{r})$ is the angle between the local nematic director **n** and the magnetic field of the NMR spectrometer.

The chiral agent added to the deuterated nematic liquid crystal compound 4'-pentyl-4-cyanobiphenyl (5CB-βd_2) is a mixture of equal weight percentages of two chiral compounds CB15 and CE2 (EM Industries). The chiral additives CB15, an isotropic liquid at room temperature, and CE2, a solid at room temperature, have a pitch length p at ambient temperatures of 0.13 and 0.1 μm, respectively, and when added to 5CB in equal weight, percentages result in a room temperature chiral nematic. The pitch length of the resulting chiral nematic is calculated by $1/p = (C_{\mathrm{CE2}}/p_{\mathrm{CE2}}) + (C_{\mathrm{CB15}}/p_{\mathrm{CB15}})$, where $C_{\mathrm{CE2}}(C_{\mathrm{CB15}})$ is the weight fraction of CE2 (CB15) in the total mixture of 5CB+CE2+CB15. The compounds were mixed in the isotropic phase to ensure a homogeneous mixture. The total weight percentage of the chiral agent in 5CB was varied between 0% and 45%, Cylindrical cavities with radii R of 0.1 μm in 60 μm thick alumina (Al_2O_3) membranes (Anopore membranes [17,18] were filled with these mixtures. Untreated alumina surfaces give tangential (planar) anchoring conditions. To ensure complete filling the strips were left to soak in the mixture in the isotropic phase overnight. The excess liquid crystal was removed from the membrane surface with Wathan filter paper and subsequently fifty 5 mm wide Anopore membrane strips were stacked exactly on top of each other. The sample was then carefully placed in a NMR sample tube, which was mounted in the spectrometer in the desired sample orientation.

III. THEORY

Assuming that the anchoring is tangential with all directions in the surface plane equivalent, the total free energy of the confined liquid crystal is expressed as

$$\begin{aligned} F = \int [& \tfrac{1}{2}K_{11}(\nabla\cdot\mathbf{n})^2 + \tfrac{1}{2}K_{22}(\mathbf{n}\cdot\nabla\times\mathbf{n} + q)^2 \\ & + \tfrac{1}{2}K_{33}(\mathbf{n}\times\nabla\times\mathbf{n})^2 \\ & - \tfrac{1}{2}K_{24}\nabla\cdot(\mathbf{n}\times\nabla\times\mathbf{n} + \mathbf{n}\nabla\cdot\mathbf{n})]dV \\ & + \tfrac{1}{2}\int W_\theta \sin^2\theta \, dS . \end{aligned} \tag{2}$$

Here K_{11}, K_{22}, and K_{33} are the conventional splay, twist, and bend bulk elastic constants, respectively, and K_{24} is the saddle-splay surface elastic constant. The nematic director is described by **n** and the chirality of the compound is incorporated in $q = 2\pi/p$, where p is the pitch length of the chiral nematic mixture. The mixture is assumed to be homogeneous throughout the cavity such that $q \neq q(\mathbf{r})$. The last term describes the interfacial free energy using Rapini-Papoular form [19]. W_θ is the out-of-plane anchoring strength (also polar anchoring strength) and θ is the angle between the nematic director and the surface. To keep the analysis simple, only first derivatives [20] of the nematic director are taken into account; therefore another surface elastic term, known as the mixed splay-bend K_{13} term, has been neglected in our calculations. The first integral is taken over the volume of the cylinder, whereas the second one is taken over the boundary. In cylindrical cavities with planar anchoring without a preferred direction, the nematic director field aligns along the cylinder axis. The parallel-axial (PA) configuration [Fig. 1(a)], a nondeformed structure, is no longer stable for chiral nematics. In the systems presented here the chiral additive leads to small deviations.

Let us first examine structures where the twist of the director field occurs along the radius, resulting in a twisted configuration, with concentric cholesteric surfaces. In the center of the cylinder the director is parallel to the cylinder axis and progressively twists approaching the cylinder surface. We shall denote it as the radially twisted axial structure [Fig. 1(b)]. This configuration contains a twist-bend deformation and is described by $\mathbf{n} = \mathbf{e}_\varphi \sin\alpha(\rho) + \mathbf{e}_z \cos\alpha(\rho)$, where α is the angle between the local nematic director and the symmetry axis of the cylinder. Substituting the expression for the nematic director into Eq. (2) and integrating over cylindrical coordinates φ and z results in the following expressions for the free energy in terms of α:

$$\begin{aligned} F_{\mathrm{RTA}} = \pi l \int \Bigg[& K_{22}\left(\frac{d\alpha}{d\rho} + \frac{1}{\rho}\sin\alpha\cos\alpha + q\right)^2 \\ & + K_{33}\frac{1}{\rho^2}\sin^4\alpha \Bigg] \rho \, d\rho - \pi l K_{24}\sin^2\alpha(R) . \end{aligned} \tag{3}$$

Here l is the cylinder length, which is assumed to be much greater than the radius R, so in the surface integral

we have neglected the contribution from bottom and upper surfaces. Minimizing the free energy for this configuration leads to the Euler-Lagrange equation, which is a nonlinear second-order differential equation

$$\frac{d^2\alpha}{d\rho^2}+\frac{1}{\rho}\frac{d\alpha}{d\rho}-\frac{1}{4\rho^2}\sin 4\alpha - \frac{2K_{33}}{K_{22}}\frac{1}{\rho^2}\sin^3\alpha\cos\alpha+\frac{2q}{\rho}\sin^2\alpha=0\ , \quad (4)$$

with the boundary condition

$$\left[\frac{d\alpha}{d\rho}+\frac{1}{\rho}\left[1-\frac{K_{24}}{K_{22}}\right]\sin\alpha\cos\alpha+q\right]_{\rho=R}=0\ . \quad (5)$$

The equation was solved by the relaxation method for ordinary differential equations and the integral for F_{RTA} was obtained by numeric integration. For fixed values of K_{24} the free energy as a function of q has a sawtooth shape, in agreement with the results of Lequeux and Kleman [8]. This dependence for equal elastic constants $K_{22}=K_{33}=K$ is shown in Fig. 2. Except for the first few peaks, the maxima and the minima of the free energy for different ratios K_{24}/K are at the same values of the product qR. The distance between maxima or minima $\Delta(qR)=\pi$ deviates from π for less than 1% over the entire range where it was calculated. There is a qualitative difference in the shape of $F_{\mathrm{RTA}}(q)$ for two different regimes of the ratio K_{24}/K: for this ratio less than 0.36 the first derivative of F_{RTA} with respect to q is continuous at the maximum points, while for larger ratios there are discontinuous changes of the slopes at the maxima (Fig. 2).

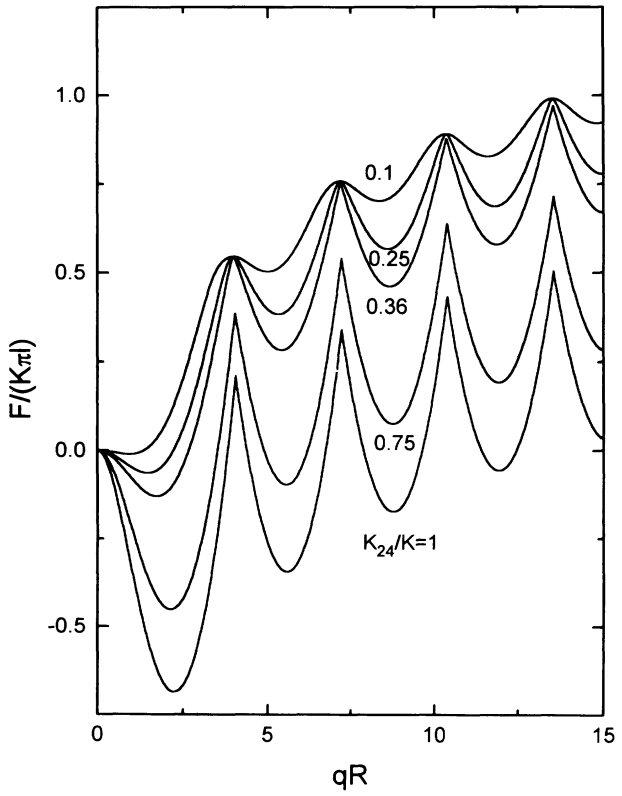

FIG. 2. Free energy of the RTA configuration as a function of chirality parameter for different values of the saddle-splay surface elastic constant K_{24}. The values of K_{24}/K for the curves from top to bottom are 0.1, 0.25, 0.36, 0.75, and 1.00.

The nematic structures in cylindrical cavities with the planar director field reveal the planar bipolar (PB) configuration [13] in each plane perpendicular to the cylinder axis. It was previously calculated that the PB configuration in the one-constant approximation has a lower free energy than the structure with a planar concentric director field [13]. We therefore conclude that also for chiral nematics a structure analogous to that of the planar-bipolar configuration exists within these cavities. To satisfy the intrinsic twist, we expect that the structure must be twisted along the cylindrical axis. When calculating the nematic director field for the ATPB configuration, the assumption is made that the solution for this configuration is separable into the PB structure within the plane and a perfect helicoidal twist of the symmetry axis of the PB along the cylinder axis [Fig. 1(c)]. The PB configuration contains a splay-bend deformation and, in cylindrical coordinates, is described by $\mathbf{n}=\mathbf{e}_\rho\cos\Psi(\rho,\varphi')+\mathbf{e}_\varphi\sin\Psi(\rho,\varphi')$, where Ψ is the angle between the local nematic director $\mathbf{n}$ and the radial vector $\mathbf{r}$ in the plane and φ' is the angle between the radial vector and the symmetry axis of the structure. For the ATPB configuration [Fig. 1(c)] we set $\varphi'=\varphi-q'z$, where φ is the angle of the radial vector with respect to the laboratory x axis and $q'z$ is the actual twist of the chiral nematic along the cylindrical axis [Fig. 1(d)]. The actual twist parameter q' is not necessarily equal to the natural parameter q. Taking into account equal elastic constants ($K_{11}=K_{22}=K_{33}=K$) and the periodicity $\Psi(\rho,\varphi'+2\pi)=\Psi(\rho,\varphi')$, the free energy [Eq. (2)] can be integrated over z to yield

$$F_{\mathrm{TPB}}=\tfrac{1}{2}Kl\int\int\left[\frac{1}{\rho^2}\left[1+\frac{\partial\psi}{\partial\varphi'}\right]^2+\left[\frac{\partial\psi}{\partial\rho}\right]^2+\left[q'\frac{\partial\psi}{\partial\varphi'}+q\right]^2\right]\rho\,d\rho\,d\varphi' + \tfrac{1}{2}W_\theta Rl\int\cos^2\psi\,d\varphi'\ . \quad (6)$$

Minimizing the free energy [Eq. (6)] results in the partial differential equation for the angle ψ

$$\frac{\partial}{\partial\rho}\left[\rho\frac{\partial\psi}{\partial\rho}\right]+\rho\left[\frac{1}{\rho^2}+(q')^2\right]\frac{\partial^2\psi}{(\partial\varphi')^2}=0\ , \quad (7)$$

with the boundary condition

$$\left[K\frac{\partial\psi}{\partial\rho}-W_\theta\sin\psi\cos\psi\right]_{\rho=R}=0\ . \quad (8)$$

The equation was solved by the overrelaxation method. For $q'=0$ the solution corresponds to the PB configuration of nonchiral nematics:

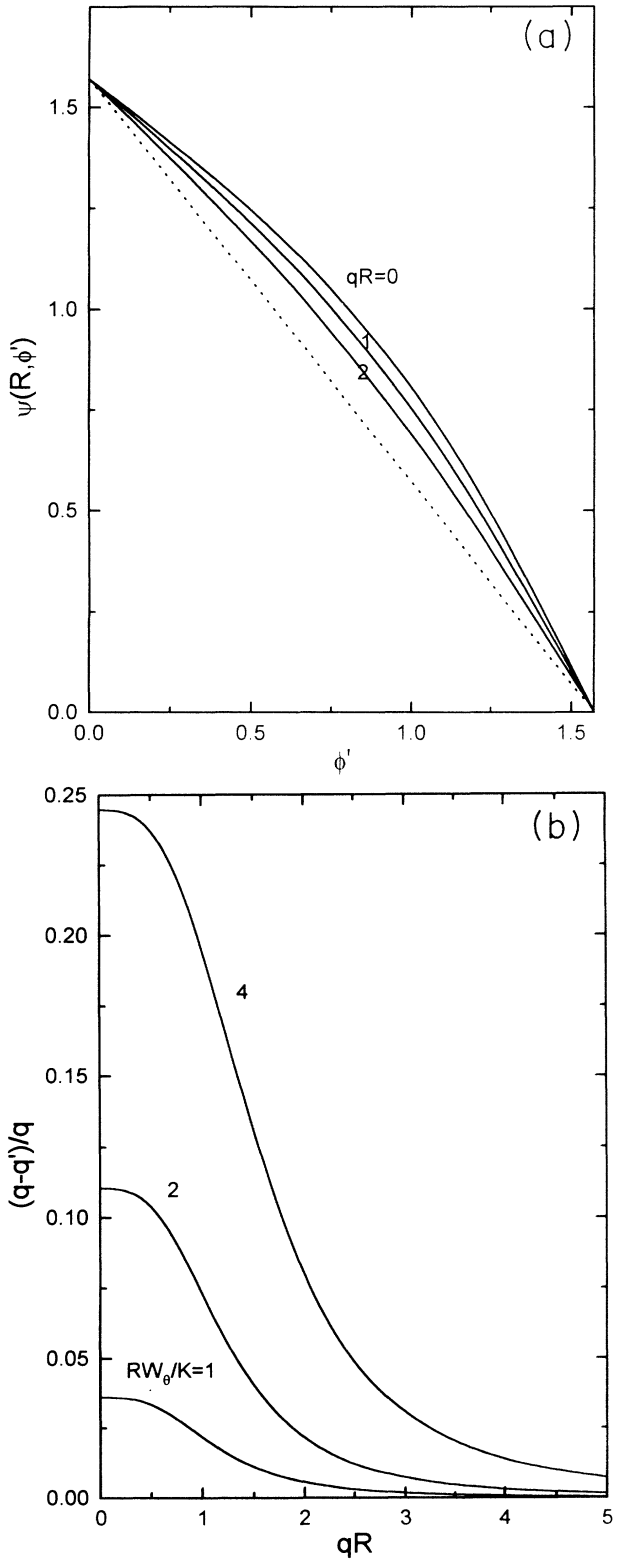

FIG. 3. ATPB configuration. (a) Nematic director angle Ψ on the cylinder boundary ($\rho=R$) as a function of polar angle φ' for $RW_\theta/K=2$ and three different values of qR; from top to bottom $qR=0,1,2$; the dotted line indicates the limit of infinite qR. (b) Relative difference between the actual and natural inverse pitch as a function of natural inverse pitch for different values of the surface anchoring strength. The values of RW_θ/K for the curves from top to bottom are 4, 2, and 1.

$$\psi(\rho,\varphi')=\arctan\left[\frac{R^2+\gamma\rho^2}{R^2-\gamma\rho^2}\cot\varphi'\right] \tag{9}$$

where

$$\gamma=\sqrt{\xi^2+1}-\xi,\quad \xi=\frac{2K}{RW_\theta}\ . \tag{10}$$

For small q' the deviation of Ψ from its nonchiral value at definite coordinates ρ and φ' is a quadratic function of q'. For $q'>1/R$ the deviation of Ψ becomes significant and is largest at the cylinder boundary [Fig. 3(a)]. For very large twist parameter q' the director field is practically everywhere oriented in the direction of the symmetry axis and the whole structure is helical, as in the unconfined chiral nematic. The actual parameter q' is found in a second minimization of the free energy. For RW_θ/K up to the value 4, the difference between q and optimal q' is small [Fig. 3(b)]. The greatest relative differences $(q'-q)/q$ are obtained in the limit of small q: up to 25% for $RW_\theta/K=4$ and $q\sim0$. The actual parameter q' is always smaller than the natural parameter q. The difference between them is negligible for qR greater than 5. But the error made by calculating the free energy with the approximation $q'=q$ is small in the whole range of parameters in our case ($0\le RW_\theta/K\le4$ and $0\le qR<\infty$). The greatest relative difference is approximately 1%. So in that range the free energy can be ap-

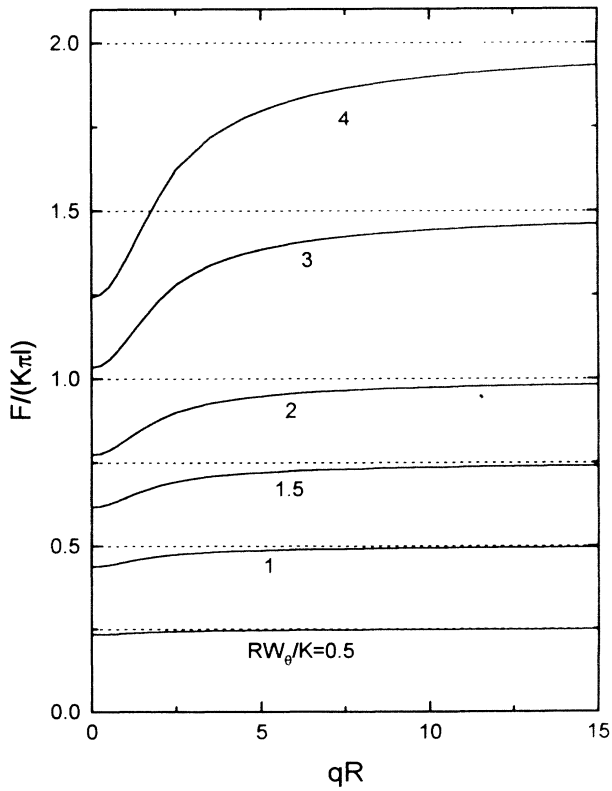

FIG. 4. Free energy of the ATPB configuration as a function of chirality parameter for different values of the surface anchoring strength. The values of RW_θ/K for the curves from top to bottom are 4, 3, 2, 1.5, 1, and 0.5. Dotted lines show the high chirality limit of the free energy.

proximately calculated by setting $q'=q$. For $q=0$ the free energy has the value, which corresponds to the nonchiral nematic,

$$F=\pi Kl[-\ln(2\gamma\xi)+(1-\gamma)/\xi] , \quad (11)$$

while for large q it approaches the limiting value due to only the surface term

$$F=\tfrac{1}{2}\pi W_\theta Rl . \quad (12)$$

The free energy as a function of twist parameter for different values of surface anchoring strength is shown in Fig. 4.

Finally the phase diagrams showing the stability of both phases in the qR-RW_θ/K plane for different values of K_{24} were calculated (Fig. 5). For small values of qR, the free energy of the radially twisted axial configuration can be negative depending on the value of K_{24}, while the free energy of the twisted planar bipolar configuration is always positive. So up to the value of the twist parameter where the free energy of the RTA structure changes sign (denoted as q_0), the RTA structure is always stable, regardless of W_θ. The larger the ratio of K_{24}/K, the larger the value of q_0. For $q>q_0$ the stability of the structures depends also on W_θ. The energy term with K_{24} lowers the free energy of the RTA configuration and stabilizes it.

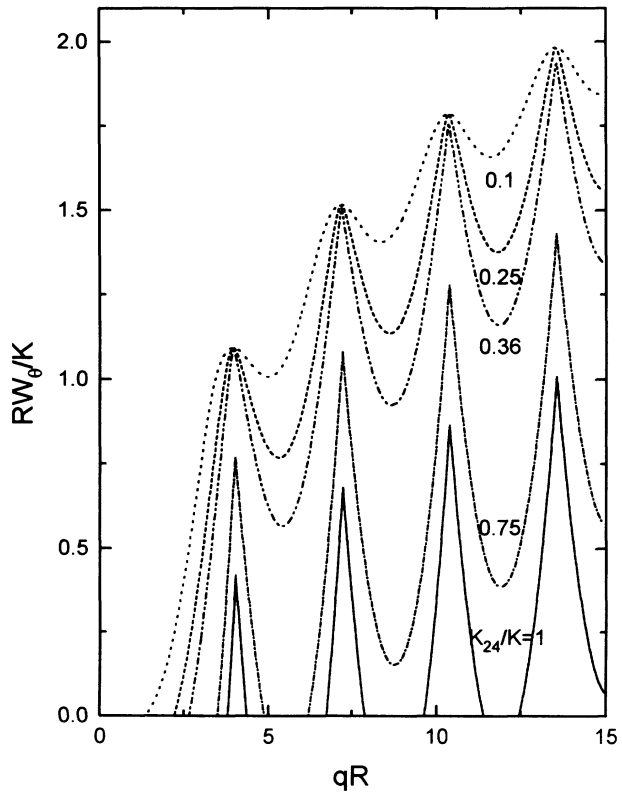

FIG. 5. Phase diagrams of the stability of the two configurations for different values of the saddle-splay surface elastic constant. The values of K_{24}/K for the curves from top to bottom are 0.1, 0.25, 0.36, 0.75, and 1.00. In each case the ATPB configuration is stable above the line and the RTA configuration below.

In the weak anchoring regime ($RW_\theta/K<1$) and for K_{24} comparable to K, a periodic reentrance from radially to axially twisted phase is predicted with increasing qR. Phase diagrams for several values of K_{24}/K are shown in Fig. 5.

IV. RESULTS

Deuterium NMR spectra for the chiral nematic liquid crystal mixtures confined to the cylindrical cavities ($R=0.1$ μm) of the alumina membranes are shown in Fig. 6. For the nonchiral nematic structure ($p=\infty$ at $C=0\%$) two sharp lines [Fig. 6(a)], separated by $\delta\nu$ at $\theta_B=0°$ and by $\frac{1}{2}\delta\nu$ at $\theta_B=90°$ (θ_B is the angle between the magnetic field and cylindrical axis), are observed. This is a (PA) structure, where the director field is oriented along the cylindrical axis [Fig. 1(a)]. For small percentages ($C<10\%$) of the chiral additive ($p=1.13$ μm at $C=10\%$) in bulk 5CB [Fig. 6(b)], the spectra are similar to those of the PA configuration. A more detailed comparison of these NMR spectra shows broadening of the spectral lines and a reduction of the quadrupole splitting. The broadening and smaller splitting of the peaks can be completely ascribed to the appearance of the twisted axial structure [Fig. 1(b)] described in Sec. III. Comparison of the NMR spectra of the PA structure [Fig. 6(a)] and the RTA structure [Fig. 6(b)] shows that in the latter the quadrupole splitting is about 20% smaller. According to Eq. (1) the nematic director of this structure exhibits a ra-

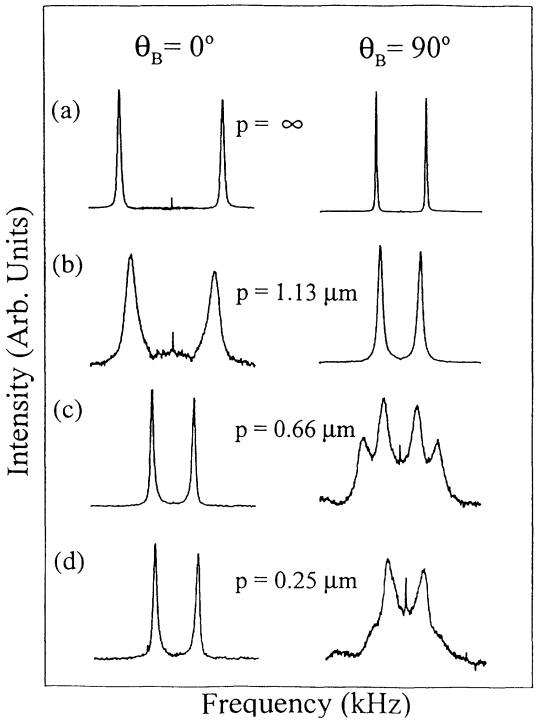

FIG. 6. Experimental NMR spectra of the chiral nematic liquid crystal mixture confined to untreated alumina membranes, when magnetic field is parallel ($\theta_B=0°$) and normal to the cylinder axis ($\theta_B=90°$): (a) PA configuration ($p=\infty$), (b) RTA configuration ($p=1.13$ μm), (c) ATPB configuration ($p=0.63$ μm), and (d) ATPB configuration ($p=0.25$ μm).

dial twist of approximately 30° at the cylinder boundary. From this information and the value of the pitch ($p=1.13$ μm, $qR=1.1$), the ratio $K_{24}/K\sim 0.1$ is estimated.

For larger percentages ($C>18\%$) of chiral additive in the bulk 5CB ($p=0.63$ μm at $C=18\%$) the spectra show two narrow peaks separated by $\frac{1}{2}\delta\nu$, indicating a perfectly planar configuration [Figs. 6(c) and 6(d)]. The cylindrical powder pattern observed for the cylinder axis perpendicular to the field ($\theta_B=90°$) is a result of all angles being equally represented in a plane. For a cylindrically confined nematic phase, such a pattern would occur in the case of planar anchoring with a concentric preferred direction of unaligned planar-bipolar director fields [15]. The spectra are also consistent with an axially twisted planar-bipolar configuration, which accommodates the inherent twist in the chiral nematic. Combining the fact that for $C>18\%$ the ATPB configuration is stable with the phase diagram (Fig. 5), we get another conformation that $K_{24}\sim 0.1\pm 0.1$.

Taking into account that the transition from RTA to ATPB structures occurs at a pitch length of $p=0.63$ μm ($qR=2$) and using the above value of K_{24}, the value of the surface anchoring strength $RW_\theta/K=0.15$ is determined from the stability diagram of Fig. 5. The ^{2}H NMR study was accompanied by an optical study of the light transmission through the membranes which also allows for a verification of the transition. Due to the optical birefringence of the liquid crystal material the optical appearance of the alumina membrane ($n=1.76$) will depend on the configuration of the liquid crystal within the cavities. For the RTA structure with a relatively small twist, the liquid crystal and the alumina membrane are nearly index matched, resulting in a translucent appearance of the membrane. For an ATPB configuration the light experiences an effective index of refraction, which is mismatched with that of the alumina matrix, resulting in an opaque appearance of the membrane.

The surprisingly low value for K_{24} stimulated a reexamination of the surface anchoring. We investigate to determine whether the preferred surface anchoring in the direction of the cylindrical axis $\mathbf{k}_z$ could account for that. Here we introduce the additional parameter W_φ (azimuthal anchoring strength) and substitute the Rapini-Papoular surface free energy with a more general one $\frac{1}{2}[W_\varphi\sin^2(\phi)+W_\Theta\cos^2(\phi)]\sin^2(\Theta)$ [13]. Here Θ is the angle between the director $\mathbf{n}$ and the preferred direction $\mathbf{k}_z$ and ϕ is the angle between the $\mathbf{k}_z-\mathbf{n}$ plane and the plane defined by $\mathbf{k}_z$ and normal to the surface. In both, RTA and ATPB phases we can use the solutions of the problem obtained with the simple surface term, but the free energies must be renormalized. In the RTA phase, the effect of the additional term leads to the renormalization $K'_{24}=K_{24}-RW_\varphi$; in the ATPB phase the out-of-plane surface anchoring strength is renormalized $W'_\Theta=W_\Theta-W_\varphi$. To see if we can explain our result with the K_{24} value of 5CB ($K_{24}/K=1$ [14]), we set $RW_\varphi/K=0.9$. For the ATPB structure the resulting free energies per unit length of the cylinder for all possible values of W_φ and q lie between $0.4K\pi$ and $0.45K\pi$, while the RTA free energy at $K'_{24}/K=0.1$ and $qR=2$ is only $0.08K\pi$. So a structural transition cannot occur at this point and we must conclude that the inclusion of the azimuthal anchoring ($W_\varphi\neq 0$) term does change the previously obtained low value for the saddle-splay elastic constant K_{24}.

V. CONCLUSION

We have reported an experimental study of chiral nematic liquid crystal confined to submicrometer cylindrical cavities. Deuterium NMR spectra clearly show a configuration transition from an axial to a planar structure, upon decreasing pitch length of the chiral nematic mixture. The radially twisted axial structure is shown to exist for pitch lengths larger than 1.13 μm. For pitch lengths smaller than 0.6 μm, a planar structure exists whose planar-bipolar director field twists along the cylinder axis, the axially twisted planar-bipolar configuration. The transition points are shown to depend on the polar anchoring strength. Our results warrant a more detailed study to experimentally observe the effect of the anchoring conditions on the transition point by treating the cavity walls with different surfactants and to observe the structures of chiral nematics confined to supramicrometer capillaries with tangential or perpendicular anchoring conditions. From the structure and the stability phase diagram we discovered that the surface elastic constant K_{24} is about an order of magnitude smaller than the bulk elastic constants. We also proved that this result is not a consequence of disregarding the azimuthal anchoring. A more detailed study, where also effects of the splay-bend elastic constant and more general anchoring will be considered, is in preparation.

ACKNOWLEDGMENTS

This research was funded in part by the National Science Foundation (NSF) ALCOM Science and Technology Center under Grant NO. DMR89-20147. Deuterated materials were provided by S. Keast and M. Neubert through the Resource Facility of the ALCOM Science and Technology Center under Grant No. DMR89-20147. The experimental NMR studies were performed with the support of NSF Grant No. DMR91-20130.

[1] P. P. Crooker, Liq. Cryst. **5**, 75 (1989), and references therein.

[2] G. Cohen and R. M. Hornreich, Phys. Rev. A **41**, 4402 (1990).

[3] R. M. Hornreich and S. Strikman, Phys. Rev. A **41**, 1978 (1990).

[4] H. S. Kitzerow, P. P. Crooker, S. L. Lwok, and G. Heppke, J. Phys. (Paris), **51**, 1303 (1990).

[5] J. W. Doane, *Liquid Crystals: Applications and Uses,* edited by B. Bahadur (World Scientific, Teaneck, NJ, 1990).
[6] D. K. Yang and J. W. Doane (unpublished).
[7] P. E. Cladis, A. E. White, and W. F. Brinkman, J. Phys. (Paris) **40**, 325 (1979).
[8] F. Lequeux and M. Kleman, J. Phys. (Paris) **49**, 845 (1988).
[9] D. K. Yang and P. P. Crooker, Liq. Cryst. **9**, 245 (1991).
[10] J. Bezič and S. Žumer, Liq. Cryst. **11**, 593 (1992).
[11] J. Bezič and S. Žumer, Liq. Cryst. **14**, 1695 (1993).
[12] G. Chidichimo, Z. Yaniv, N. A. Vaz, and J. W. Doane, Phys. Rev. A **25**, 1077 (1982).
[13] R. J. Ondris-Crawford, G. P. Crawford, S. Žumer, and J. W. Doane, Phys. Rev. Lett. **70**, 194 (1993).
[14] D. W. Allender, G. W. Crawford, and J. W. Doane, Phys. Rev. Lett. **67**, 1442 (1991).
[15] A. Golemme, S. Žumer, J. W. Doane, and M. Neubert, Phys. Rev. A **37**, 559 (1988).
[16] J. W. Doane, in *Magnetic Resonance of Phase Transitions,* edited by F. W. Owens, C. P. Poole, Jr., and H. A. Farach (Academic, New York, 1979).
[17] Anotec Separations, 226 E. 54th St., New York, NY 10022.
[18] G. P. Crawford, L. M. Steele, R. J. Ondris-Crawford, G. S. Iannachione, C. J. Yeager, J. W. Doane, and D. Finotello, J. Chem. Phys. **96**, 7788 (1992).
[19] B. Jerome, Rep. Prog. Phys. **54**, 391 (1991).
[20] V. M. Pergamenshchik, Phys. Rev. E **48**, 1254 (1993).